Flow Directs Surface-Attached Bacteria to Twitch Upstream

Yi Shen,[†△] Albert Siryaporn,[‡△] Sigolene Lecuyer,[§] Zemer Gitai,[‡] and Howard A. Stone[†*]
[†]Department of Mechanical and Aerospace Engineering and [‡]Department of Molecular Biology, Princeton University, Princeton, New Jersey; and [§]Department of Molecular and Cellular Biology, Harvard University, Cambridge, Massachusetts

ABSTRACT Bacteria inhabit a wide variety of environments in which fluid flow is present, including healthcare and food processing settings and the vasculature of animals and plants. The motility of bacteria on surfaces in the presence of flow has not been well characterized. Here we focus on *Pseudomonas aeruginosa*, an opportunistic human pathogen that thrives in flow conditions such as in catheters and respiratory tracts. We investigate the effects of flow on *P. aeruginosa* cells and describe a mechanism in which surface shear stress orients surface-attached *P. aeruginosa* cells along the flow direction, causing cells to migrate against the flow direction while pivoting in a zig-zag motion. This upstream movement is due to the retraction of type IV pili by the ATPase motors PilT and PilU and results from the effects of flow on the polar localization of type IV pili. This directed upstream motility could be beneficial in environments where flow is present, allowing bacteria to colonize environments that cannot be reached by other surface-attached bacteria.

INTRODUCTION

Bacteria have evolved a number of motility mechanisms that enable movement in liquid environments and on solid or semisolid surfaces. In addition, bacteria colonize surfaces to form biofilms, which are found in natural settings and in many medically relevant and food-handling environments. A distinguishing feature of these settings is the presence of fluid motion. Although flagellar-driven swimming in liquid environments has been characterized extensively (1–5), far less is known about surface motility in these environments. For example, despite being crucial for fundamental aspects of bacterial physiology such as biofilm formation and pathogenesis, the ability of surface motility mechanisms to establish persistent motion has been seldom studied (6–8). A few studies did demonstrate that such persistent directed motion can occur in the plant pathogen *Xylella fastidiosa* (9) and the aquatic parasite *Mycoplasma mobile* (10,11) in environments where fluid flow is present. In particular, these cells migrate on surfaces against the direction of a fluid flow. This upstream movement is hypothesized to result from the aggregate effects of the bacterial motility machinery and the forces from the fluid flow (9). However, the mechanism, generality, and biological significance of such upstream motility remain unclear. Here we characterize the effect of flow on the surface movement of the ubiquitous human pathogen *Pseudomonas aeruginosa*.

P. aeruginosa is a pathogen with significant relevance to human health and disease. In particular, it forms robust biofilms and is found in environments where flow is present, such as in catheter tubes (12), intravenous lines, and the human lung and circulatory system (13). *P. aeruginosa* cells move on surfaces (14–16) through the extension and retraction of type IV pili (17,18), which are localized to the cell poles. The physiological significance of the polar localization of these pili has remained unclear. Several characteristic motions on surfaces have been observed in the absence of flow, including persistent crawls and random walks (19,20). Here we find that flow orients *P. aeruginosa* and causes a subpopulation of cells to migrate against the flow direction via a mechanism that requires retraction of type IV pili. The ability to migrate upstream could be beneficial, enabling *P. aeruginosa* to colonize environments that are inaccessible to other human pathogens that lack this surface motility.

MATERIALS AND METHODS

Strains and growth conditions

Strains were grown overnight at 37°C on LB agar plates (Sigma-Aldrich, St. Louis, MO). Colonies were inoculated in tryptone broth (10 g of Bacto Tryptone per liter of water; BD, Franklin Lakes, NJ), grown with aeration at 37°C to an optical density at 600 nm (OD_{600}) of ~1, diluted 1:10, and loaded into microfluidic devices. To test the motility of strains in the absence of glucose, cultures were grown in minimal medium A (21) with 0.2% glucose to an OD_{600} of 1, diluted 1:10 into fresh minimal medium A lacking glucose, and loaded into microfluidic devices. *P. aeruginosa* strains PA14, PA14 *pilC*::Tn5 (22), PA14 *flgK*::Tn5 (22), PA14 *pilU*::MAR2xT7 (23), PA14 *pilT*::MAR2xT7 (23), PA14 *cheA*::MAR2xT7 (23), PA14 *chpA*::MAR2xT7 (23), PA14-GFP (24), and AFS19 (PA14 Δ*pilTU*::*aacC1*) (see Materials and Methods in the Supporting Material) were used in this study.

Construction of microfluidic devices

Microfluidic devices were fabricated using soft lithography techniques (25). Polydimethylsiloxane (PDMS) channels were fabricated using the Sylgard 184 silicone elastomer kit (Dow Corning, Midland, MI) with cross-linker at a concentration of 10%. PDMS was poured onto molds created using soft lithography, cured, sealed onto cover glass (VWR, Radnor, PA), and stored

Submitted February 2, 2012, and accepted for publication May 15, 2012.

△Yi Shen and Albert Siryaporn contributed equally to this work.

*Correspondence: hastone@princeton.edu

Editor: Charles Wolgemuth.

0006-3495/12/07/0146/6 $2.00

doi: 10.1016/j.bpj.2012.05.045

at room temperature. The resulting microfluidic channels were straight with dimensions of 3-cm in length, 400-μm in width, and 30-μm in height.

Surface-shear stress assays

Microfluidic channels were injected with bacterial cultures using 1-mL syringes, given ~15 min for cells to adhere to the cover-glass surface and flushed with fresh medium using a syringe pump (Harvard Apparatus, Holliston, MA). Channels were placed on an inverted microscope and imaged at room temperature. The shear stress at the cover-glass surface was approximated using the equation

$$\sigma_S \approx \frac{6Q\mu}{wh^2},$$

where Q is the flow rate; μ is the viscosity of the bacterial solution, which is approximately equal to that of water for the concentration of bacteria used in these experiments; and w and h are the width and height of the channel, respectively. We applied flow rates of 0.5–30 μL/min which corresponds to ~0.1–10 Pa of surface shear stress.

Phase contrast and fluorescence microscopy

Microfluidic devices were imaged at room temperature through the cover glass using a model No. DMI4000 B inverted microscope, model No. HCX PL FLUOTAR PH2 40×/0.6 NA or 63×/0.7 NA objectives, and a model No. DFC 360FX camera (all by Leica Microsystems, Buffalo Grove, IL). Time-lapse movies of cells were produced by acquiring phase-contrast images at the cover-glass surface every 1–2 min for 10–16 h unless indicated otherwise. For the experiments shown in Fig. 4 *D*, images were acquired every 0.5–1 s for ~15 min.

To measure cell adhesion to the surface, cells were stained using Cy3 mono-reactive dye (GE Healthcare, Piscataway, NJ) as described in Skerker and Berg (18), resuspended in minimal medium A, loaded into microfluidic channels, and imaged using differential interference contrast (DIC) and total internal reflection fluorescence (TIRF) microscopy using a model No. Ti-E microscope (Nikon Instruments, Melville, NY), 100×/1.49 NA APO TIRF objective (Nikon Instruments), a 100-mW 532-nm diode laser (ChangChun Dragon Lasers, ChangChun, JiLin, China), 552-nm LP dichroic (Semrock, Rochester, NY), 607/70 nm emission filter (Semrock), and a Clara camera (Andor Technology, South Windsor, CT).

Cell displacement, velocity, and orientation analysis

The displacement, velocity, and orientation of individual cells were computed using our own software written in MATLAB (The MathWorks, Natick, MA). Approximately 5000–20,000 cells were analyzed in each experiment unless otherwise noted. Cell positions and orientations were computed from cell masks constructed from cell boundaries, which were determined by applying Sobel or Canny edge-detection algorithms or an image-thresholding algorithm (26) with phase-contrast images. Cell position and orientation measurements were refined by inverting phase-contrast images corresponding to the cell masks, subtracting by the average background pixel value, and computing first- and second-order image moments from grayscale values. Cell displacement was measured as the change in position of a cell from its nearest-neighbor cell in the previous image. Cells that shared the same nearest neighbor from the previous image were excluded from the analysis. The cell velocity was computed as the quotient of the displacement and the time interval between the previous image. Displacements in the same direction as the flow were taken to be positive and those in the opposite direction as the flow were taken to be negative. The upstream speed reported in Fig. 1 *E* is the average of all the negative velocities measured during 10–15 h experiments.

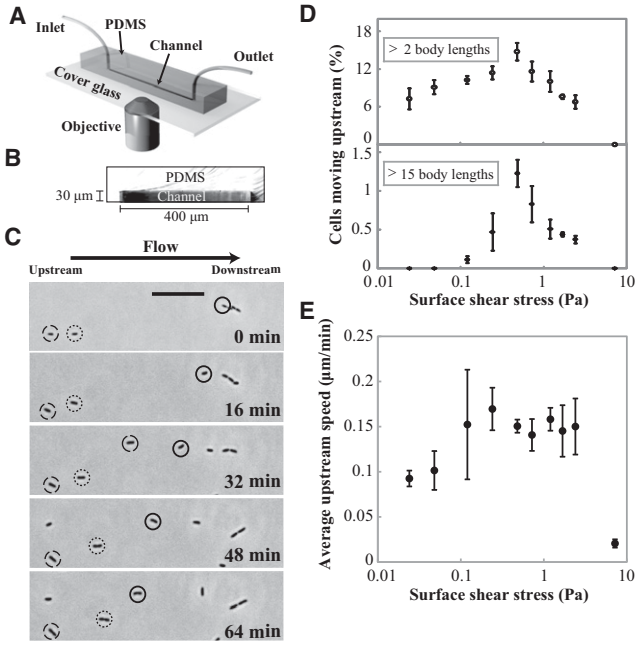

FIGURE 1 Surface-attached *P. aeruginosa* migrate against the flow direction. (*A*) Schematic of the microfluidic device used to study motility of *P. aeruginosa* under flow conditions. Cells and media are flowed through the inlet. Cells on the cover-glass surface in the microfluidic channel are imaged on an inverted microscope. (*B*) Image of the microfluidic-channel cross section. The straight channel is ~400-μm wide and 30-μm high. (*C*) Time-lapse images of cells under flow (surface shear stress ~1.3 Pa). Four different types of motion are observed. Cells slide in the same direction as the flow (*dashed circle*), are stationary (*four-arc circle*), detach from the surface (*two-arc circle*), or move in the opposite direction (*solid circle*) of the flow (scale bar: 20 μm). (*D*) Fraction of the total surface-attached cell population that moves more than two, or up to 15 cell-body lengths over a 15 h time period, as a function of surface shear stress. (*E*) Average speed of upstream migrating cells as a function of shear stress (see Materials and Methods for description of analysis). (*Data points*) Average of at least three independent experiments in panel *D* and of at least two independent experiments in panel *E*. (*Error bars*) Standard deviation.

Flow reversal

Liquid tryptone broth cultures were inoculated, grown to an OD_{600} of ~1, diluted 1:10, and loaded into microfluidic channels. After 15 min, fresh medium containing 1-μm microtracer particles (Fluoresbrite Polychromatic Micron Microspheres, Polysciences, Warrington, PA) was flowed into the channel. Surface-attached cells and beads that passed within the plane of focus were imaged at 1–2 min intervals in time-lapse movies using phase-contrast microscopy as described above. Surface-attached cells that migrated upstream were identified. After 1 h of flow, image acquisition was increased to 50-ms intervals and the flow direction of the syringe pump was reversed. The point at which flow reversal occurred was determined by measuring bead velocities, which were quantified using the cell-velocity algorithm described above.

RESULTS

We constructed a microfluidic device to continuously image the movements of surface-attached *P. aeruginosa* cells under different surface shear stresses and growth conditions (Fig. 1 *A*, and see Materials and Methods). The channel is

straight from the inlet to outlet and has a rectangular cross section that is 400-μm wide and 30-μm high (Fig. 1 *B*). We varied the flow rates in our device from 0.5 to 30 μL/min so that surface-attached cells experience shear stresses ranging from 0.1 to 10 Pa (see Materials and Methods), which are stresses typically found in catheter tubes and animal vasculature (27–29). Under these conditions, cells exhibited at least four different types of motion: 1), smooth sliding along the surface in the same direction as the flow; 2), jerky, upstream migration along the surface in the opposite direction to the flow; 3), attachment to the surface without any movement; and 4), detachment from the surface (Fig. 1 *C*, and see Movie S1 in the Supporting Material). We observed little or no sustained motion in the direction perpendicular to the flow. Cells that migrate in the direction opposite to the flow typically moved at a rate of ~0.5–1 μm/min, which corresponds to 15–30 cell-body lengths/h. These speeds are comparable to mean speeds previously reported for pilus-dependent twitching motility of *P. aeruginosa* (20).

Motivated by the observation of cell movement in the opposite direction to the flow (motion Type 2 above), we tested the hypothesis that the fluid flow directs cells upstream by examining how shear stress affects the number of cells that migrate upstream and discovered a significant differential effect on cell subpopulations. We found that the total number of cells on the surface decreased as we increased surface shear stress. However, the relative fraction of the surface population that moved upstream was largely unchanged with increasing surface shear stress (see Fig. S1 in the Supporting Material). Over the course of a 15-h experiment, we observed that the fraction of the population that moved upstream at least two body lengths increased with flow rate and reached a maximum at a flow rate corresponding to a surface shear stress of 0.5 Pa (Fig. 1 *D*, *top panel*). This effect is even more pronounced for cells that move upstream by at least 15 body lengths (Fig. 1 *D*, *bottom panel*). Shear stress thus stimulates persistent upstream migration up to 0.5 Pa. These results are consistent with a previous report showing that shear stress promotes *P. aeruginosa* adhesion to surfaces (over shorter timescales) (30). We also examined the effects of surface shear stress on upstream migration speeds and found that speeds were largely unchanged for shear stresses in the range of 0.1–3 Pa, but dropped at a critical threshold of 7 Pa (Fig. 1 *E*).

The jerky nature of the upstream migration is reminiscent of twitching motility, in which motion is driven by the extension and retraction of type IV pili (17,18). Furthermore, type IV pili are required for upstream movement in *X. fastidiosa* (9), though it remains unclear whether the role of pili in this case is to mediate adhesion of the cell with the surface, to generate the upstream driving force, or to perform both of these functions. We therefore examined the dependence of surface motility in flow using *pilC*$^-$ mutants, which are defective in the production of type IV pili (22), and *pilT*$^-$, *pilU*$^-$, and *pilTU*$^-$ mutants, which produce type IV pili but are impaired in twitching motility due to the absence of the pilus retraction motors. Upstream migration was still observed in the single-retraction motor (*pilT*$^-$ and *pilU*$^-$) mutants.

However, no upstream migration was observed for either the pilus production (*pilC*$^-$) or double (*pilTU*$^-$) mutants (Fig. 2 *A*, and see Fig. S2 and Movie S2 in the Supporting Material). In addition, *pilTU*$^-$cells detached from the surface far less frequently than wild-type cells. In time-lapse experiments where fresh medium was flowed continuously through the channel, the number of *pilTU*$^-$ cells on the surface increased with time (due to growth) and nearly saturated the surface after 10 h. In contrast, the density of wild-type cells at the surface was sparse and constant during this period (see Fig. S3). This observation suggests that pilus retraction promotes release of cells from the surface. Together, these data show that upstream migration requires retraction of type IV pili by the PilT or PilU motors.

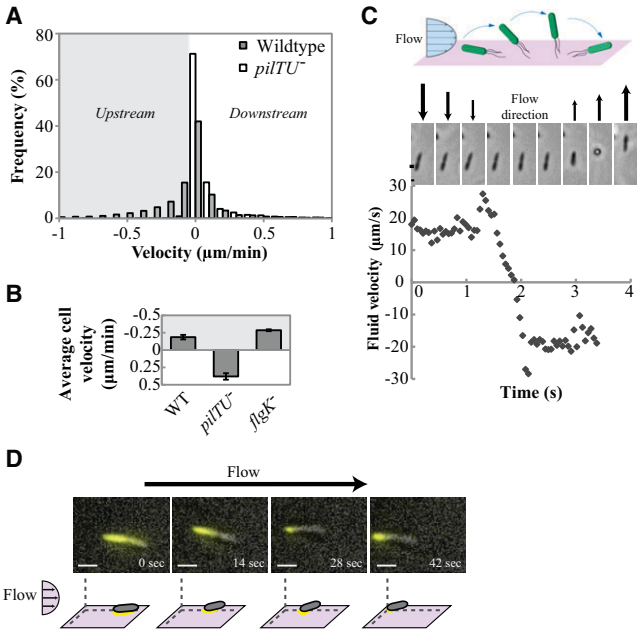

FIGURE 2 *P. aeruginosa* cells migrate upstream on a surface by retracting type IV pili. (*A*) Velocity distributions for wild-type cells and *pilTU*$^-$ cells, which lack motors to retract pili, under a flow corresponding to a surface shear stress of 0.5 Pa. Negative velocities indicate upstream movement. (*B*) Average cell velocities for motile wild-type, *pilTU*$^-$, and *flgK*$^-$ cells under a flow corresponding to a surface shear stress of 0.5 Pa (see additional Materials and Methods in the Supporting Material). (*Bars*) Average of at least two independent experiments. (*Error bars*) Standard deviation. (*C*) An upstream migrating cell stands up and flips about the upstream-facing pole after flow reversal. Flow velocity was measured using microtracer particles. Flow direction is indicated (*arrows*) above phase contrast images, which correspond approximately to their placement along the horizontal time axis. A schematic depicting cell reorientation during flow reversal appears at the top. (*D*) An upstream migrating cell adheres to the surface at the upstream-facing pole. Composite DIC and TIRF images of fluorescently labeled cell bodies (see Materials and Methods, scale bar: 2 μm) (*top*) and schematic (*bottom*). (*Yellow highlighting* in the *schematic*) Portion of the cell that adheres to the surface.

We observed upstream migration in *flgK* cells, which are defective in the production of flagella, demonstrating that this motion does not require flagella (Fig. 2 *B*) and is not directly related to the flagella-based mechanism of upstream swimming in fluid environments (4,5,31). Furthermore, the motion is unlikely due to chemotaxis because chemical gradients are negligible for the flow rates used in these experiments. To support this conclusion, we performed experiments with *cheA* (see Movie S1) and *chpA* (data not shown) mutants, which lack chemoreceptors, and experiments using a minimal media that lacks glucose (see Movie S1). In all of these cases, we continued to observe upstream migration.

To rationalize the upstream direction of surface migration, we note that type IV pili are localized at the poles of the bacteria (22,32). Thus, the flow should cause any cells attached to the surface by type IV pili to pivot about the pole and align cells along the flow direction with type IV pili at the forward-facing pole (Fig. 2 *C*). Any subsequent pilus retraction leads to upstream movement. In support of this model, we found that reversing the flow direction causes upstream-migrating cells to flip about the upstream-facing cell pole (Fig. 2 *C*). In contrast, *pilC*$^{-}$ cells are almost never observed to flip after flow reversal (see Movie S3). Furthermore, cells adhere to the surface only at the upstream-facing pole as they move upstream (Fig. 2 *D* and see Movie S4).

We examined the orientation of cells in the plane of the cover-glass surface (Fig. 3 *A*). In the absence of flow, cells are randomly oriented (Fig. 3, *B* and *C*). Within minutes of initiating flow, most cells become oriented toward the flow direction (Fig. 3, *B* and *C*). Furthermore, the degree of alignment with the flow axis increases monotonically with shear stress (Fig. 3 *D*), which confirms that the flow directs cell orientation. However, cells do not align perfectly with the flow direction, which suggests that cells exert a force with a component that is perpendicular to the flow direction. Type IV pili, which are distributed radially at cell poles, could produce such a force. This hypothesis is supported by the result that *pilC*$^{-}$ mutants, which lack type IV pili, are more aligned with the flow direction than wild-type cells (Table 1).

Because pili pull cells both against and across the flow direction, cells should move diagonally upstream. Indeed, analysis of the upstream migration reveals that the motion is not simply unidirectional but instead exhibits characteristic diagonal zig-zag movements (Fig. 4, *A* and *B*, and see Movie S5). Specifically, we observe short diagonal runs whose orientation angle oscillates about the flow axis over the course of minutes (Figs. 1 *C* and 4, *A* and *C*). Changes in the orientation angle are also observed over the course of several seconds, which suggests that the extension and retraction of pili occurs on this timescale (Fig. 4 *D*). As yet further support for the dependence of upstream twitching on type IV pilus retraction, the zig-zag movements we observe in the presence of flow are consistent with the twitching-based slingshot cell motions recently observed under no-flow conditions (33). No such changes in orientation angle are observed in *pilTU*$^{-}$ mutants, which demonstrates the dependence of this motion on the active retraction of type IV pili. We can also now rationalize the critical shear-stress threshold of 7 Pa (Fig. 1 *E*), noting that the surface force on the bacterial body (area $= A \approx 1–2 \times 10^{-12}$ m^2) is ~10–15 pN (= 7 Pa × A). As previous studies place the lower bound on the retraction force of a single pilus at 10 pN (18), our data suggest that the force for upstream migration is generated by the retraction of only a few pili.

DISCUSSION

There are many settings in which bacteria colonize surfaces in the presence of flow, such as those found in healthcare settings and in the vasculature of plants and animals. The effects of flow on bacterial motility could thus play a significant role in health and disease. We have demonstrated that flow directs *P. aeruginosa* cells to move upstream and that this motility requires retraction of type IV pili.

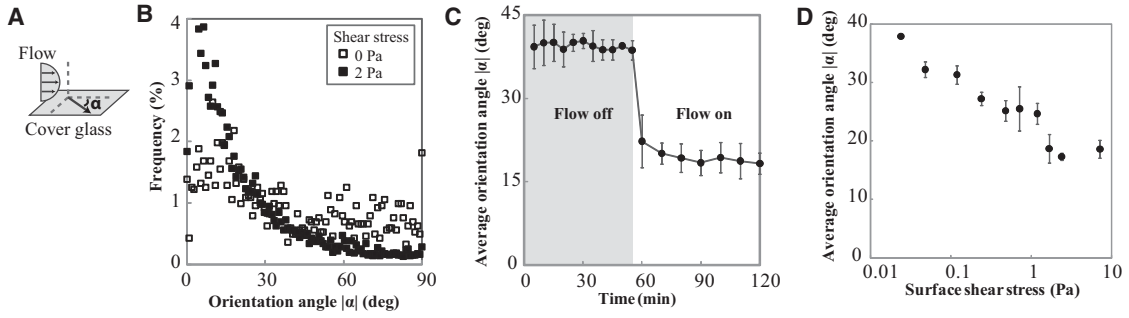

FIGURE 3 Flow aligns cells along the flow direction. (*A*) Schematic depicting the orientation angle α on the cover-glass surface. (*B*) Distribution of cell orientation angles in the presence and absence of flow. Cells are oriented in random directions in the absence of flow. The bias toward the flow direction is a remnant of the procedure used to load cells into the channel. (*C*) A step change in flow induces cell alignment toward the flow direction. (*D*) Orientation of cells as a function of shear stress. (*Data points* in panels *C* and *D*) Average of at least three independent experiments. (*Error bars*) Standard deviation.

TABLE 1 Strains defective in pilus function, which are more aligned with the flow direction

Strain	Average orientation angle $\|\alpha\|$ (deg)
wt	26.5 ± 4.3
flgK$^-$	24.5 ± 3.3
pilTU$^-$	17.5 ± 1.2
pilC$^-$	13.8 ± 1.9

Average of the absolute value of the orientation angle relative to the flow direction was computed for wild-type and mutant strains. A flow rate corresponding to 0.5 Pa of surface shear stress was used. Errors represent the standard deviation of at least three independent experiments. The term "wt" is wild-type.

Our results provide direct evidence for a mechanism in which cells are oriented toward the flow direction with the anchoring pole positioned upstream. This orientation results from the asymmetric nature of the cell attachment (Fig. 2, *C* and *D*) and the effects of flow on such a system. The localization of type IV pili at the cell poles, rather than uniformly along the cell body as in the case of type I pili and fimbriae, is likely to be important for upstream motility. Thus, our findings suggest that localizing type IV pili at the cell pole provides a selective advantage by endowing cells with the ability to move upstream. The mechanism for upstream twitching mediated by polar type IV pili is based on the fact that the pili both mediate the attachment between the cell and surface and provide the driving force for motility. Flow rotates polar-attached cell bodies about the anchoring pole so that the pole faces upstream. Through the extension and retraction of the radial type IV pili, cells pivot against the flow direction with a side-to-side motion. Although flow appears to be a key factor, our experiments do not rule out an additional biological role in determining cell orientation.

Upstream twitching appears to be a generic tactic response of cells with polar type IV pili to flow and thus may be present in a wide range of other bacteria. The results appear to be generalizable to bacteria that attach to surfaces at cell poles and possess colocalized motility machinery. This behavior is consistent with rheotaxis, which is defined as directed motion due to flow. Indeed, rheotactic behavior has been observed in the freshwater bacterium *M. mobile* (10), which possesses motility machinery localized toward a cell pole.

We highlight two additional features of upstream twitching. First, we found that typically only a fraction of the cell population migrated upstream (Fig. 2 *A*). This raises an interesting question of whether *P. aeruginosa* cells are differentiated into distinct cell fates—such as those that move upstream and those that detach and move with the flow. Such behavior would enable a bacterial population to explore both upstream and downstream environments. Second, the zig-zag motion observed in cells migrating upstream could be advantageous in densely packed environments such as a biofilm. A natural consequence of this motion is that cells explore a larger area of the surface than those that move along a straight path. Indeed, in high-cell-density experiments, we frequently observed upstream-migrating cells moving around nonmotile cells (see Movie S6).

Upstream twitching could enable cells with polar type IV pili to preferentially colonize upstream environments. Consequently, the upstream-directed migration of bacteria due to flow may play a significant role in settings relevant to infection and contamination, where surface-attached bacteria encounter flow environments.

SUPPORTING MATERIAL

Additional Materials and Methods, three figures, and six movies are available at http://www.biophysj.org/biophysj/supplemental/S0006-3495(12)00625-X.

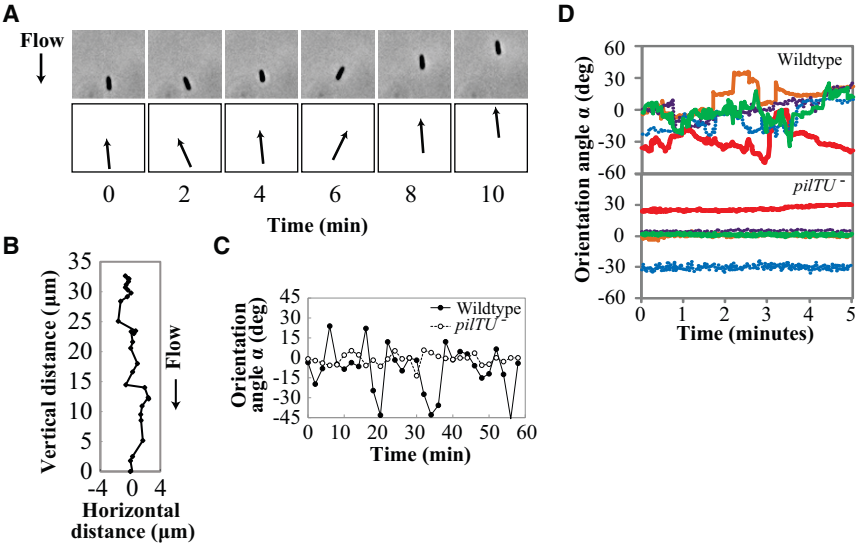

FIGURE 4 (*A*) Phase-contrast images of a cell moving upstream in a flow corresponding to 0.5 Pa. The cell orientation and approximate position is indicated (*arrows* below the images). (*B*) Trace of a typical cell migrating upstream under a flow corresponding to a surface shear stress of 0.5 Pa. The interval between each time point (*solid circle*) is 2 min. Cell orientation as a function of time for wild-type and *pilTU*$^-$ cells at (*C*) 2-min and (*D*) 1-s image acquisition intervals. Traces are shown for five different cells for each strain in *D*.

We thank J. Shaevitz, N. Wingreen, and other members of the biofilm reading group for insightful comments, A. Persat for feedback on flow effects, K. Cowles for helpful discussions on motility, S. van Teeffelen for helpful discussions on image analysis, H. Berg for bringing to our attention his work on motility of *Mycoplasma*, and members of the Gitai and Stone groups for suggestions.

This work was supported by Princeton University (to H.A.S.), the National Institutes of Health New Innovator award No. 1DP2OD004389-01 (to Z.G.), and the National Institutes of Health Center for Quantitative Biology grant No. P50GM071508 (for A.S.).

REFERENCES

1. Berg, H. C. 1975. Chemotaxis in bacteria. *Annu. Rev. Biophys. Bioeng.* 4:119–136.
2. Blakemore, R. 1975. Magnetotactic bacteria. *Science.* 190:377–379.
3. Manten, A. 1948. Phototaxis in the purple bacterium *Rhodospirillum rubrum*, and the relation between phototaxis and photosynthesis. *Antonie van Leeuwenhoek.* 14:65–86.
4. Hill, J., O. Kalkanci, …, H. Koser. 2007. Hydrodynamic surface interactions enable *Escherichia coli* to seek efficient routes to swim upstream. *Phys. Rev. Lett.* 98:068101.
5. Kaya, T., and H. Koser. 2012. Direct upstream motility in *Escherichia coli*. *Biophys. J.* 102:1514–1523.
6. Bertrand, J. J., J. T. West, and J. N. Engel. 2010. Genetic analysis of the regulation of type IV pilus function by the Chp chemosensory system of *Pseudomonas aeruginosa*. *J. Bacteriol.* 192:994–1010.
7. Whitchurch, C. B., A. J. Leech, …, J. S. Mattick. 2004. Characterization of a complex chemosensory signal transduction system which controls twitching motility in *Pseudomonas aeruginosa*. *Mol. Microbiol.* 52:873–893.
8. Miller, R. M., A. P. Tomaras, …, M. L. Vasil. 2008. *Pseudomonas aeruginosa* twitching motility-mediated chemotaxis towards phospholipids and fatty acids: specificity and metabolic requirements. *J. Bacteriol.* 190:4038–4049.
9. Meng, Y. Z., Y. X. Li, …, H. C. Hoch. 2005. Upstream migration of *Xylella fastidiosa* via pilus-driven twitching motility. *J. Bacteriol.* 187:5560–5567.
10. Rosengarten, R., A. Klein-Struckmeier, and H. Kirchhoff. 1988. Rheotactic behavior of a gliding mycoplasma. *J. Bacteriol.* 170:989–990.
11. Miyata, M., W. S. Ryu, and H. C. Berg. 2002. Force and velocity of mycoplasma mobile gliding. *J. Bacteriol.* 184:1827–1831.
12. Stamm, W. E. 1991. Catheter-associated urinary tract infections: epidemiology, pathogenesis, and prevention. *Am. J. Med.* 91(3B):65S–71S.
13. Hoiby, N. 1974. *Pseudomonas aeruginosa* infection in cystic fibrosis. Relationship between mucoid strains of *Pseudomonas aeruginosa* and the humoral immune response. *Acta Pathol. Microbiol. Scand. B Microbiol. Immunol.* 82:551–558.
14. Henrichsen, J. 1983. Twitching motility. *Annu. Rev. Microbiol.* 37: 81–93.
15. Wall, D., and D. Kaiser. 1999. Type IV pili and cell motility. *Mol. Microbiol.* 32:1–10.
16. Mattick, J. S. 2002. Type IV pili and twitching motility. *Annu. Rev. Microbiol.* 56:289–314.
17. Merz, A. J., M. So, and M. P. Sheetz. 2000. Pilus retraction powers bacterial twitching motility. *Nature.* 407:98–102.
18. Skerker, J. M., and H. C. Berg. 2001. Direct observation of extension and retraction of type IV pili. *Proc. Natl. Acad. Sci. USA.* 98:6901–6904.
19. Gibiansky, M. L., J. C. Conrad, …, G. C. Wong. 2010. Bacteria use type IV pili to walk upright and detach from surfaces. *Science.* 330:197.
20. Conrad, J. C., M. L. Gibiansky, …, G. C. Wong. 2011. Flagella and pili-mediated near-surface single-cell motility mechanisms in *P. aeruginosa*. *Biophys. J.* 100:1608–1616.
21. Miller, J. H. 1992. A Short Course in Bacterial Genetics: A Laboratory Manual and Handbook for *Escherichia coli* and Related Bacteria. Cold Spring Harbor Laboratory Press, Plainview, NY.
22. O'Toole, G. A., and R. Kolter. 1998. Flagellar and twitching motility are necessary for *Pseudomonas aeruginosa* biofilm development. *Mol. Microbiol.* 30:295–304.
23. Liberati, N. T., J. M. Urbach, …, F. M. Ausubel. 2006. An ordered, nonredundant library of *Pseudomonas aeruginosa* strain PA14 transposon insertion mutants. *Proc. Natl. Acad. Sci. USA.* 103:2833–2838.
24. Rusconi, R., S. Lecuyer, …, H. A. Stone. 2011. Secondary flow as a mechanism for the formation of biofilm streamers. *Biophys. J.* 100:1392–1399.
25. Qin, D., Y. Xia, and G. M. Whitesides. 2010. Soft lithography for micro- and nanoscale patterning. *Nat. Protoc.* 5:491–502.
26. Miyashiro, T., and M. Goulian. 2007. Single-cell analysis of gene expression by fluorescence microscopy. *Methods Enzymol.* 423: 458–475.
27. Karino, T., H. L. Goldsmith, …, Y. Sohara. 1987. Flow patterns in vessels of simple and complex geometries. *Ann. N. Y. Acad. Sci.* 516:422–441.
28. Giddens, D. P., C. K. Zarins, and S. Glagov. 1990. Response of arteries to near-wall fluid dynamic behavior. *Appl. Mech. Rev.* 43:S98–S102.
29. Krams, R., J. J. Wentzel, …, C. J. Slager. 1999. Effect of catheter placement on 3-D velocity profiles in curved tubes resembling the human coronary system. *Ultrasound Med. Biol.* 25:803–810.
30. Lecuyer, S., R. Rusconi, …, H. A. Stone. 2011. Shear stress increases the residence time of adhesion of *Pseudomonas aeruginosa*. *Biophys. J.* 100:341–350.
31. Marcos, H. C., H. C. Fu, …, R. Stocker. 2012. Bacterial rheotaxis. *Proc. Natl. Acad. Sci. USA.* 109:4780–4785.
32. Cowles, K. N., and Z. Gitai. 2010. Surface association and the MreB cytoskeleton regulate pilus production, localization and function in *Pseudomonas aeruginosa*. *Mol. Microbiol.* 76:1411–1426.
33. Jin, F., J. C. Conrad, …, G. C. Wong. 2011. Bacteria use type-IV pili to slingshot on surfaces. *Proc. Natl. Acad. Sci. USA.* 108:12617–12622.